university of groningen / faculty of science and engineering / biomedical engineering

Quantification of Perfusion in QASPER Phantom using Pulsed Arterial Spin Labelling

Seshasai Ganesan (S3381196)
Department of Biomedical Engineering
University of Groningen
Email: sesha2000watts@gmail.com
Period: 01/05/2020 – 22/01/2020

Supervisor: Dr. Remco Renken
Medical Physicist,
MRI Centrum, Antonius Deusinglaan 1, UMCG
9713 AV Groningen
Email: r.j.renken@umcg.nl

Mentor: Dr. Antoon T.M. Willemsen,
Department of Nuclear Medicine and Molecular Imaging, UMCG
9713 AV Groningen
E-mail: a.t.m.willemsen@umcg.nl

Thesis submitted in fulfilment of requirements for the degree of Master's in Biomedical Engineering Specializing in Diagnostic Imaging and Instrumentation.

Declaration:

I, Seshasai Ganesan declare that the project titled “Quantification of Perfusion with QASPER Phantom using Pulsed Arterial Spin Labelling”, is an original work and I am the sole author of this and that every technique and literature borrowed has been referenced wherever needed.

Signature: 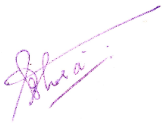

Date: 22/01/2020

Table of Contents

Acknowledgment:
I would like to thank my supervisor dr Remco Renken for the support and guidance provided during the whole course of this project. Given the situation the data provided to me by dr R.J.H.Borra was of great help in order to conclude the research. I would also like to thank Remco for the regular weekly meetings and for the time and help provided during my final month which was very hectic.

1.0 Abstract:

In this research project, the Arterial Spin Labelling technique was used to study and quantify perfusion and the reproducibility of the values in the Quantitative Arterial Spin Labelling Perfusion Reference (QASPER) Phantom. The FAIR PASL incorporating the QUIPSS II saturation pulse technique was used for labelling of the spins. The perfusion was quantified using the widely accepted PASL CBF formula ad parameters, presented in the white paper for ASL Implementation. Voxel wise analysis of the Phantom was done in the different perfusion discs and the perfusion values based upon different flow rate settings of 100, 200, 300, 400, 450, and 485 ml/min were calculated and compared. The results showed that with the parameters set for the experiment, while they were in the acceptable range according to the white paper, there were large deviations and a high degree of over quantification of the perfusion than stated in the phantom documentation. An increasing trend in the values of the perfusion was observed for each flow rate in every disc. The flow dynamics within the phantom layers was also studied to justify the results in the trend. While the results did not concur with the values stated in the phantom documentation, further modifications of the ASL technique and understanding of transit times in the phantom may be helpful in improving the results of this study.

2.0 Introduction:

The main goal of this study is to check feasibility of the PASL technique to quantify perfusion in the QASPER phantom and to analyze the results for improving the use of the technique for future use.

2.1 Literature Review:

Magnetic Resonance Imaging, is a widely used non invasive imaging technique to visualize images of the anatomy(Hawkes et al., 1980). They are used in the medical field for diagnosis, treatment and pathology identification. It works on the principle of proton spins of the body being aligned using a powerful magnet which employs a main magnetic field(B0) to align the spins in the same direction as the B0 field. When an RF pulse(B1) is applied perpendicular to B0, the proton spins align in the direction of B1 which leads to the net magnetization being tipped away from B0. The RF pulse is then turned off and MR signal, is acquired as the protons relax back to align with the main magnetic field is detected. As the protons have spin, it has an angular momentum due to which, the spins precess around B0. The velocity of this precession is the Larmour Frequency , which is proportional to the field strength. The figure 1: (Grover et al., 2015)below depicts precession of a proton.

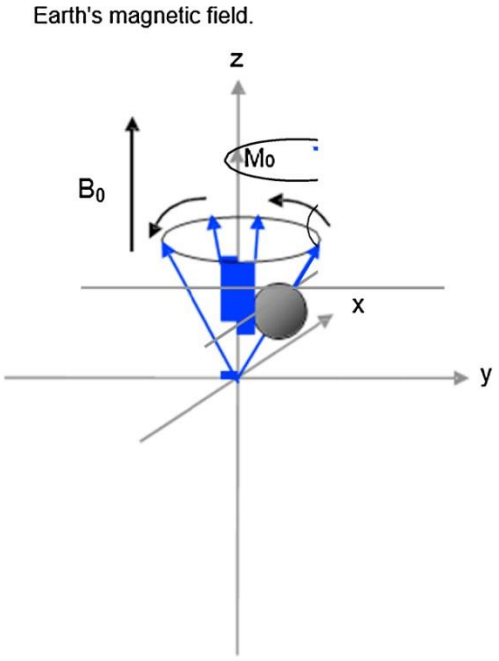

Figure 1: Precession of Spins around Main Magnetic Field Bo

These resonant protons give off signal when the B1 field is removed which causes relaxation and realignment of the protons with B0 (i.e) magnetic vector goes back from Mxy to Mz. Different tissues have different rates of relaxation which leads to the difference in the signal acquired by the MRI receiver coil. There are two types of relaxation namely,

1. T1 relaxation (Berger, 2002)which is the spin lattice relaxation. As this occurs, energy is dissipated to the lattice. T1 is the time for the spins to return to 63% of their original energy.
2. T2 relaxation (Berger, 2002) or spin spin relaxation, is caused by the dephasing of the spins after the RF pulse has been applied, resulting in more randomness of the alignment of the spins due to dephasing.

2.3 Perfusion MRI:

Oxygen delivery is critical to the body functions and the brain uses approximately 20% of oxygen (Jahng et al., 2014). The regulation of blood flow and oxygen delivery through the blood is thus a critical aspect and understanding of this is important to identify and study various pathologies. The blood flow is mostly constant due to vascular resistance which dilates or relaxes the vessels based upon the necessity of blood flow to a region. This depends upon the metabolic oxygen demand (Fantini et al., 2016) of the cells. Perfusion can be described in biological terms, as the delivery of blood to the tissues for the purpose of oxygenation and nutrients. It is normally measured in milliliters per hundred grams per minute (Rosen et al., 1990). Perfusion MRI is a non invasive technique to study the cerebral haemodynamics. There are two broad techniques that are employed based upon the use with or without a contrast agent and they are,

1. With Exogenous Contrast

    - Dynamic Susceptibility MRI(DSC-MRI)
    - Dynamic Contrast Enhanced MRI(DCE-MRI)
    3. Without Exogenous Contrast: Arterial Spin Labelling Techniques.

2.3.1 DSC-MRI:

DSC-MRI is one of the most widely used techniques to measure human brain perfusion. DSC images are based upon a bolus which consists of a Gadolinium contrast (Jahng et al., 2014). A T2 weighted image after the passage of the bolus creates a signal which is plotted versus time to produce the Arterial Input Function (Stadler et al., 2017). The contrast bolus causes a drop in intensity as illustrated in the figure:2 (Calamante, 2010) as it passes through a particular region. This causes decrease in the local magnetization and hence, the signal of that region to drop during its transit. A signal intensity vs time curve can be generated from this and parameters like blood-flow, mean transit time (MTT) can be derived using which a voxel to voxel basis analysis can be done to create perfusion maps. Although widely used, this technique has its disadvantages. Depending upon the deconvolution algorithm, the delay of the bolus can lead to underestimation of flow and error in calculating the MTT (Calamante et al., 2000). This can lead to underestimation of the perfusion. Another cause of error for absolute quantification of the perfusion is the relaxation rate of the contrast agent and the MR signal which is assumed to be linear which is not true. Dispersion of Bolus also leads to underestimation of the CBF. Another issue arises due to the poor resolution of the DSC-MRI technique which causes partial volume effects (van Osch et al., 2003). Furthermore, the relaxivity of the MR signal and the contrast agent is assumed to be uniformly spread across the different tissues. Because different tissues have varying number of vessels, the relaxivity can also be different, which can lead to systematic errors.

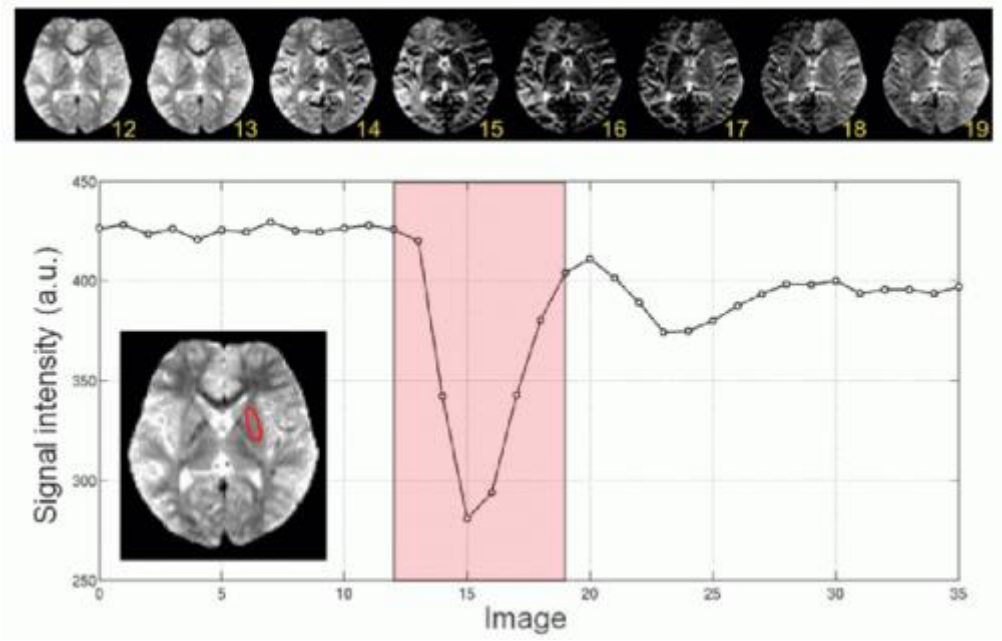

Figure :2: DSC-MRI technique showing signal drop with bolus passage

2.3.2 DCE-MRI:

DCE-MRI is another contrast based method. Unlike DSC-MRI which depends upon T2 relaxation, in this method, the haemodynamic signals depend upon the T1 relaxation. A collection of rapid T1 weighted images are used to get the changes in the signals that is induced by the T1 shortening effect due to the paramagnetic nature of the contrast agent. Like DSC, this is also used to get a time intensity curve where the signal changes reflect the blood flow, which can be calculated using appropriate compartment kinetic models. One of the most often used model is the Tofts model, and is shown in fig:3 (Chikui et al., 2012). It assumes that the contrast agent is at equilibrium between the extra and intracellular space and plasma. DCE-MRI is extensively used to study tumours like pleural mesothelioma as DCE-MRI exposes patients to no radiation . This technique suffers from a few caveats like image artifacts (Parker et al., 2000). Like DSC-MRI, this also suffers from partial volume effects due to its low resolution. Furthermore, depending upon the accuracy of the kinetic model being used for quantification (Buckley, 2002), many systematic errors are introduced.

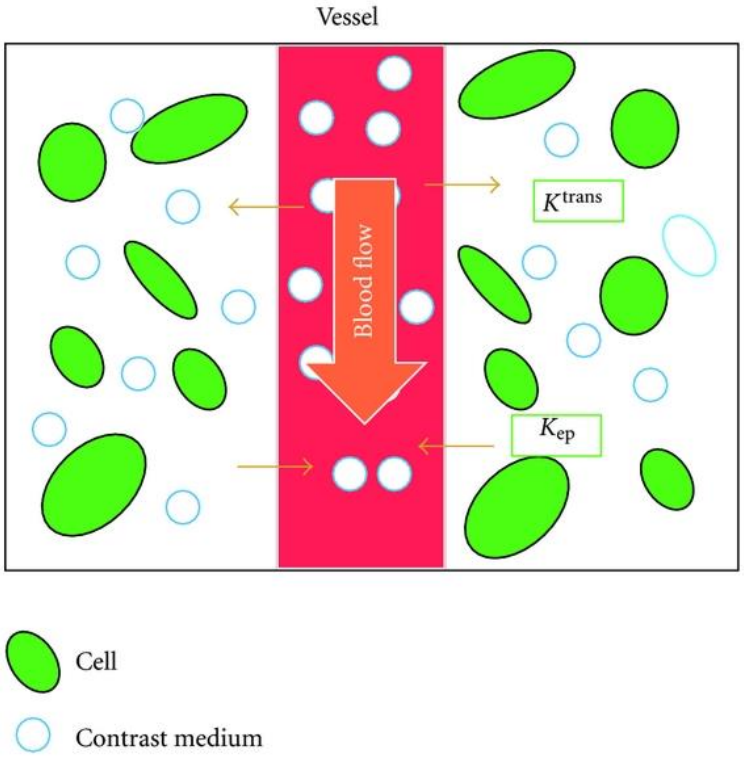

Figure:3 Toft's Model

2.3.3 Arterial Spin Labelling:

Arterial Spin Labelling is a non invasive, non ionizing MR technique to measure perfusion using intrinsic diffusers (Alsaedi et al., 2018). This method is carried out through the labelling of the H atoms of the arterial water by means of RF pulses. The resulting inversion of the longitudinal magnetization of the blood, upstream the region of interest, causes a drop in the local magnetization measured in the imaging plane. The method was first conceived about 25 years ago when research was done on rats to measure their cerebral blood flow using water as the tracer (Williams et al., 1992). Due to its non invasive nature, it has been used to study perfusion in individuals who have poor renal functions and in need of repetitive follow ups (Nery et al., 2020). The basic goal of the ASL technique is to quantify the perfusion of blood to a region of specific tissue voxels, by producing flow labelled images and a control image where the static tissue signals are identical, but the blood that is flowing in has a different magnetization. With the application of an RF pulse, the arterial blood is inverted in one or both label and control images, before entering the imaging region. This causes a local decrease in the magnetization and therefore the signal in the imaging plane due to these inverted spins as illustrated in figure:4. Only very small amounts of the inverted arterial blood water accumulate as the relaxation time for water is around 2 seconds. This leads to very low signal to noise ratios as the signal is very low compared to that of the static tissues. The control and label images are normally taken in interleaved fashion and then are subtracted to get the signal difference which roughly reflects on the perfusion that is proportional to the blood flow. ASL has found its use in many clinical applications like paediatric studies where it serves as an attractive option for studying cerebral perfusion due to its safety and ethical aspects compared to nuclear medicine where problems like the retention of the radionuclide in the patient can prove to be hazardous and due to radiation risks in infants. Studies have shown that there is decreased CBF in children diagnosed with sickle-cell anaemia (Gevers et al., 2012), which showed promise in future studies in the possible diagnosis of further risk of stroke in children. ASL has also been applied to study the occlusion of the cerebral arteries and its effects. Another important contribution of ASL is the identification of tumours which other contrast MR techniques cannot establish due to the blood brain barrier (Tiwari et al., 2017). Other areas of research that ASL has contributed includes epilepsy, depression, Rett syndrome and Alzheimer's (Zhang et al., 2017).

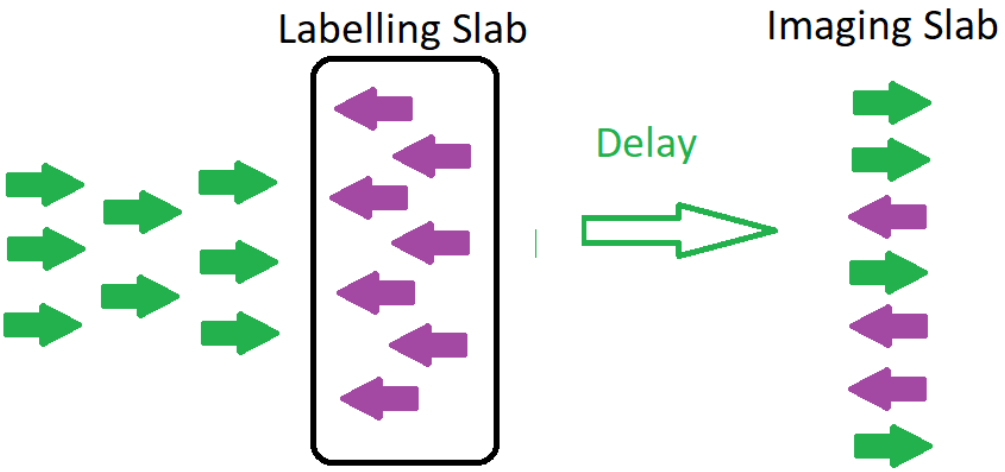

Figure :4 Diagram roughly depicting spin inversion. The green arrows indicate the spins that have not been inverted. The purple arrows indicate the labelled spins. The labelled signals after reaching the imaging slice cause a drop in the total magnetization while relaxing with T1. Note: Spins maybe tagged in Label and/or Control images.

Four techniques have been developed based upon the labelling process

1. Continuous Arterial Spin Labelling (CASL)
2. Pulsed Arterial Spin Labelling (PASL)
3. Pseudo Continuous Arterial Spin Labelling (PCASL)
4. Velocity Selective Arterial Spin Labelling (VSASL)

CASL:

This technique developed by Williams, Detre (Williams et al., 1992), involves the continuous application of RF pulses for 2-4 seconds coupled with slice selection gradient in the direction of flow. This induces adiabatic inversion that is flow driven. Inversion of the blood magnetization, takes place in a very narrow plane normally upstream the imaging plane. Because of the continuous RF pulse, CASL has a higher SNR than the other techniques (Wang et al., 2002). But the continuous RF pulse also leads to a high specific absorption rate(SAR) and magnetization transfer(MT) effects, with the latter leading to over estimation of perfusion. The long off resonance RF pulse of CASL, saturates the macromolecules due to their broad frequency spectrum. When this pool of macromolecules enter the imaging slice, the magnetization gets transferred to the water bound protons and saturates static tissue-signal. This leads to an increase in the signal in the difference images which leads to over quantification. There have been many implementations of CASL until now to tackle these effects. The very first solution shown in fig:5(a) was using another inversion pulse exactly opposite to the labelling plane during the control session. This induces similar MT effects in the imaging slice which gets nullified when obtaining the subtracted image. But this technique resulted in an even higher SAR due to the application of two continuous RF pulses. The second modification shown in fig:5(b) was using two inversion pulses through sinusoidal modulation placed very close to each other due to which the magnetization inverted by the first plane gets uninverted as it passes the second plane thereby the MT effects cancel each other (D C Alsop & Detre, 1998). The two inversions act as 360^{o} pulses. Other techniques used are Simultaneous Proximal Distal Radio Frequency irradiation. As stated above the SAR is further increased by these methods due to two RF pulses and additional coils cannot be implemented to avoid MT effects due to hardware compatibility issues. Spins are inverted with a labelling efficiency ranging from 80-98%.

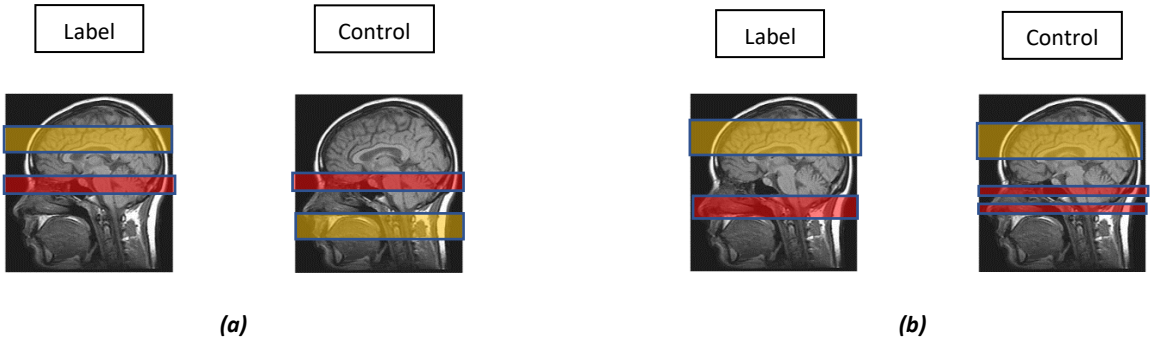

Fig 5: Solution to overcome the MT Effects in CASL. The red slabs represent the inversion pulses and the yellow slab represents the imaging slab.

PASL:

Proposed in 1994 by (Edelman et al., 1994), this technique uses short RF pulses between 5 and 20 milliseconds over a broad labelling slab of about 10 cm thickness to invert the blood proximal to the imaging plane. The signal is acquired after an appropriate labelling delay and the difference between the signals measured with and without labelling gives an estimate of the perfusion. Because of the ease of application and lower SAR, this method is preferred nowadays over CASL for perfusion imaging. Depending upon this labelling zone, there are two types , symmetric and asymmetric methods. One of the symmetrical methods called Flow Alternating Inversion Recovery(FAIR) (Kim, 1995) used in this research study is shown in Fig:6(a). It uses an inversion pulse which is non selective in the control condition. In the label, an additional slice selection is given which, as shown in the fig:6. This sequence uses a narrow inversion plane for the label image while the the control image has no slice selection thereby inverting the whole plane. Non symmetrical methods include the first PASL sequence being the EPISTAR (fig:6(b)) which has a labelling zone of is about 10-15 mm in thickness located above and below the imaging volume for control and label respectively(Ferré et al., 2013). This inversion slab is provided after saturation of magnetization in the imaging slice in the label along with spoiler gradients. In the control, the spoiler gradient is applied and the inversion slab is on the opposite side downstream to the imaging volume. IN the label, the same is applied along with a 90 ^{o} pulse. This induces similar MT effects which gets cancelled out while subtracting. To compensate for the MT effects, many modifications have been done to improve the labelling slice profile like PICORE (Proximal Inversion with Control of Off-Resonance Effects), Q2TIPS and QUIPSSII(Wong et al., 1998) for reducing the sensitivity of arterial transit time(ATT) (Luh et al., 1999). The arrival times of the spins to each voxel as well as controlling the temporal width of the bolus is a major issue in quantification of PASL data. The QUIPSSII technique used in this research described in the figure:7 is a solution to the above stated problem of bolus width. The tagging plane, leads to a temporally poorly defined bolus, as the physical width of the bolus is controlled by the labelling plane but the temporal width of the bolus is dependent upon the flow velocity. This results in the volume of the tagged blood being more for higher flow rates/CBF and vice versa. Hence, the labelled blood is first allowed to enter the imaging slab and after time TI1, a saturation pulse (QUIPSS II pulse, green peak in figure:7) is applied very close to the imaging slab to saturate any further spins that flow in(tail end of bolus). This leads to a well defined temporal length of the bolus which is now well defined irrespective of the flow velocity.

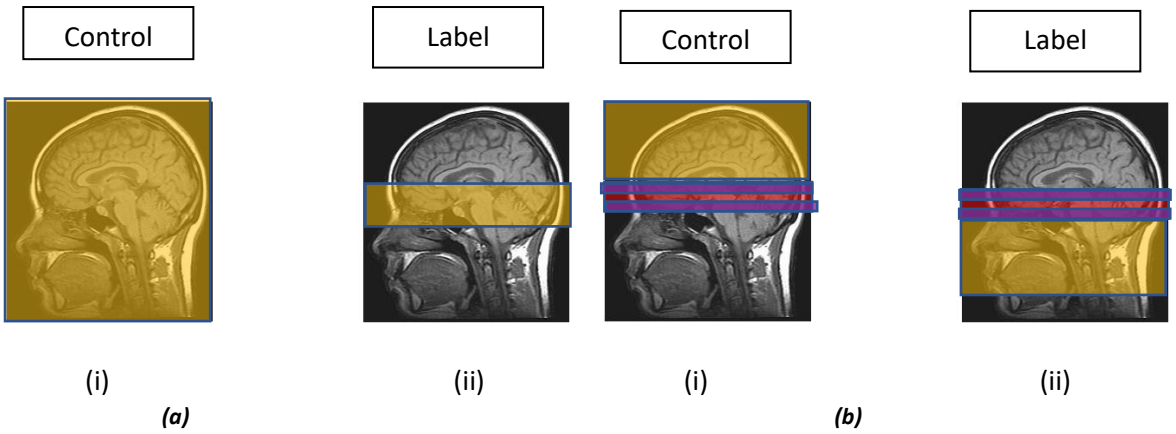

Fig:6 The FAIR PASL technique (a-i) shows the control where a non selective pulse inverts the whole plane and (a-ii) is the label image which has a small inversion plane. EPISTAR technique shows control (b-i) where 90 degree spoiler shown in purple is applied to both control and label. The red plane is the imaging plane. The 180 degree inversion slabs in yellow are on the opposite sides for control and the label is applied with a slice selective 90 degree saturation pulse with spoiler gradients

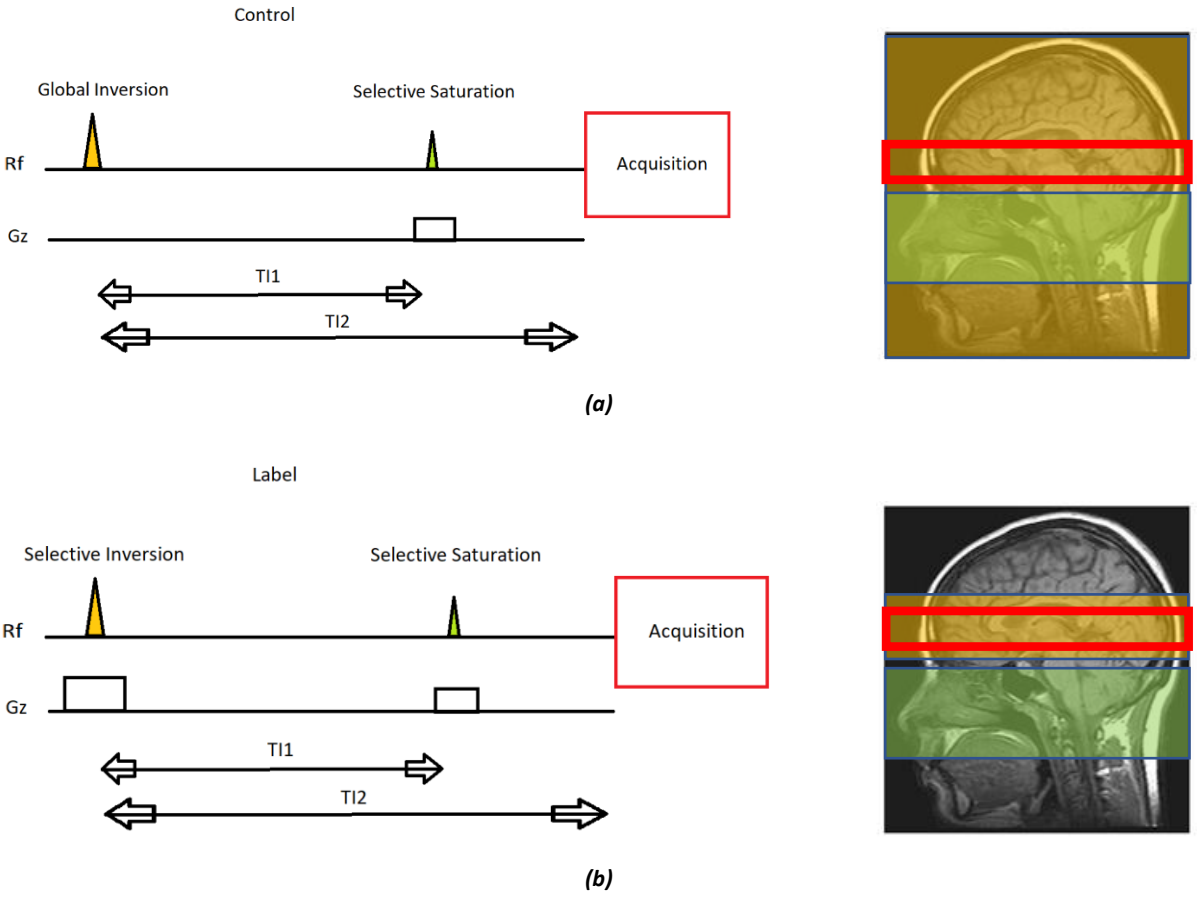

Fig:7 QUIPSS II addition to the FAIR sequence. (a)Control & (b) Label. The red outline indicates the imaging plane, the green block in the pulse sequence and the diagram indicates the QUIPSS II saturation slab and the yellow block indicates the inversion slab.

PCASL:

Pseudo Continuous Labelling was a method that was develop by Dai and colleagues(Dai et al., 2008)which tackled the effect of long during RF pulses present in the CASL sequence. This technique uses several RF pulses of around 0.5 milliseconds lasting our 1.5 seconds and combines the advantages of CASL and PASL. Similar to CASL, it also uses a narrow labelling plane. Signal loss is minimized by tagging just below the imaging plane. It is also the recommended implementation strategy currently (David C Alsop et al., 2015), due to its ease of compatibility with MR hardware and due to its superior efficacy of labelling, lower SAR and high SNR.. Similar to CASL, PCASL is based upon flow driven adiabatic inversion which requires the flow velocity to be high enough for adiabatic conditions to be satisfied. The tagging efficiency is also higher than CASL due to better control over the MT effects.

VSASL:

In this technique, tagging is based upon the velocity of the blood and the location of the labelling. With the transit time posing a major challenge in the above mentioned techniques , in VS-ASL, the labelling occurs throughout the whole area and not just the interest imaging slab and hence without the presence of a transit time. The tag pulse is velocity selective and a cut off is provided, to ensure that inversion occurs only above this cut off velocity occurs irrespective of the location. The images that are acquired after delay are the magnetization of the spins that have slowed down into tissues and micro-vasculatures. This decrease in magnetization signal is proportional to the flow velocity.

2.4 Flow Quantification Models in ASL:

The raw ASL images must be computed and processed to provide CBF/Perfusion maps which are then qualitatively and quantitatively evaluated. There are two models that are used to quantifying ASL data.

1. T1 Model
2. General Kinetic Model

2.4.1 T1 Model:

This model was not used in this research study and has been explained just to outline the quantification calculations in general as it has been used in the past. It is a model that was introduced by (Williams et al., 1992) which includes flow effects to a modified Bloch equation according to the Ficks Principle which states that the flow is proportional to the difference in the delivery and clearance of a tracer being the water bound protons from a voxel

$$dM(t)/dt = (M0 - M(t))/T1 + fMa(t) - fMv(t) \text{ where,} \ldots\ldots\ldots\ldots (1)$$

M0 is the longitudinal equilibrium magnetization of tissue.

Ma ,Mv and M are longitudinal magnetizations of the arterial, venous and tissue blood

As mentioned, the flow is basically reflected by the difference image which gives an idea of the delivered magnetization. This magnetization difference with respect to equilibrium magnetization (M0) gives an idea of the effect of this flow on apparent relaxation time T1app. Thus it can be said that the flow delivers a magnetization which is

$$M\_in = f \cdot M0a \cdot dt$$

and it also clears

$$M\_out = f \cdot Mv \cdot dt$$

Two assumptions are considered for the correlation between blood and tissue magnetizations. First assumption is that the brain tissue is a compartment which is given by,

$$Mv(t)=M(t)/\lambda$$

Where λ describes the equilibrium distribution of the tracer in the blood and tissue. The next assumption is that M0a which is the arterial blood magnetization when fully relaxed, equals M0/ λ in equilibrium. The change in magnetization due to flow f, is then given by,

$$dM(flow) = M\_in - M\_out \Rightarrow f \cdot M0a(t) - f \cdot Mv(t) = (M0 - M(t)) \cdot f \cdot dt/\lambda$$

$$dM(t)/dt = (M0 - M(t))/T1 + (M0 - M(t)) \cdot f/\lambda$$

The labelled blood also causes a decrease in M0 which is time dependent and with an apparent T1 constant T1 app. The magnitude of T1app depends upon T1 and is given by,

$$1/T1\ app = 1/T1 + f/\lambda$$

In steady state flow, the flow is given by,

$$f = (\lambda/T1\ app) \cdot (Mcontrol - Mlabel)/(2Mcontrol)) \quad .....(2)$$

2.4.2 General Kinetic Model:

The above model mentioned gives an idea of the flow with relation to the exchange of magnetization between static tissue and the labelled blood but not systematic errors like the variability in the transit time, exchange of the tagged water between the tissues and surrounding capillaries which can impact the T1 and also clearance of the tagged water from these capillaries (Buxton et al., 1998). The GKM model takes into account these factors to give a more general model. This model considers the signal difference as the measure of the tracer magnetization concentration delivered due to the flow into the tissues which retains this magnetization. This time dependent magnetization will depend upon the flow and clearance and also the longitudinal magnetization.

This can be described by defining functions for each voxel shown as shown below,

1. AIF(t), which is the arterial input function that denotes the delivery of the intrinsic agent (labelled blood in this case) to the voxel(s) of interest.

2.The residue function R(t).

The above mentioned GKM model using the two above stated parameters can in general be put together as a convolution of the two functions.

$$\Delta M(t) = f\ X\ AIF(t) * Rt) \text{ .....(3)}$$

$$\Delta M(t) = f\ X\ \int_0^0 AIF(t)R(t-t')dt') \text{.....(4)}$$

The above functions can be considered for calculations under three main assumptions of the bolus arrival/transit time. The incoming labelled bolus signal which is also the AIF(t), normally takes the shape of a box car/top-hat function. The length of this function is defined in a pCASL sequence as the labelling duration. However, for PASL the labelling duration is generally not well defined due to limited spatial extent of the coil. For this reason, the QUIPSS II and Q2TIPS is applied. Due to T1 relaxation, the label decays as it reached the imaging plane and this drop must be accounted for in the AIF. In pCASL this is not an issue as the bolus is labelled at the exact distance from the imaging slice whereas for PASL, due to the width of the labelling plane, the distal part of the tagged bolus takes longer and arrives with a more decayed T1. The magnitude of AIF can be defined in terms of the labelled concentration. This is related to the equilibrium magnetization M0a of arterial blood. ASL being subtraction images of Control and Label, the magnitude becomes 2 timesM0a. An assumption is made, that there is no labelled blood that arrives to a voxel before transit time Δt and once it arrives, the tagged bolus keeps arriving until the whole duration of the bolus from Δt to Δt+τ. While taking the tagging efficiencies of PASL and pCASL into consideration, the AIF is shown below in equation:5,

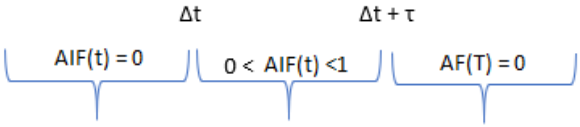

Fig:8 Depicts the arterial input function is non zero only within the interval Δt < t < Δt + τ

$$AIF(t) = \begin{cases} 0 & 0<t<\Delta t \\ 2M0\alpha e^{-\left(t/T_{1b}\right)} & \text{for PASL} \quad \Delta t<t<\Delta t+\tau \\ 2M0\alpha e^{-\left(\Delta t/T_{1b}\right)} & \text{for CASL} \\ 0 & \end{cases} \text{.....(5)}$$

t is the bolus duration which can be known after application of QUIPSS II pulse. α is the inversion efficiency which is 0.98 for PASL and 0.83 for pCASL.

The residue function is the amount of magnetization left when the bolus arrives at a particular voxel. It is assumed that the labelled bolus remains in the region and is based upon another assumption, that the labelled blood water is exchanged with the tissue. Alongside this process, there is decay with T1.

$$R(t) = e^{-t/T1}$$

The above equations can be put in equation:5 and rearranged after convolution, to calculate the perfusion f, denoted generally by the cerebral blood flow(CBF).

$$CBF = \frac{6000 \cdot .\Delta M \, .e^{\left(TI/T_{1a}\right)}}{2 \cdot \alpha . TI1 . M0a} \qquad \text{for QUIPSSII PASL.....(6)}$$

$$CBF = \frac{6000 \cdot \Delta M \, .e^{\left(PLD/T_{1a}\right)}}{2 \cdot \alpha . TI1 . M0a\left(1 - e^{\left(TI/T_{1a}\right)}\right)} \qquad \text{for PCASL.....(7)}$$

The value 6000 is a conversion factor from ml/g/s to ml/100g/min. With regards to M0a, it cannot be calculated using simple subtraction of the difference image. Normally, a proton density weighted image is acquired, with a long TR and this is used to quantify the M0 for the tissue. The proton density of blood is different from tissue. Hence a correction is to be introduced based upon the blood tissue partition coefficient λ.

M0a=M0/λ..

Substituting this in equation(6) & (7), we get

$$CBF = \frac{6000 \cdot \lambda . \Delta M \, .e^{\left(TI/T_{1a}\right)}}{2 \cdot \alpha . TI1 . M0} \qquad \text{for QUIPSSII PASL.....(8)}$$

$$CBF = \frac{6000 \cdot \lambda . \Delta M \, .e^{\left(PLD/T_{1a}\right)}}{2 \cdot \alpha . TI1 . M0\left(1 - e^{\left(TI/T_{1a}\right)}\right)} \qquad \text{for PCASL.....(9)}$$

3.0 Methodology:

In order to quantify the blood flow, the QASPER flow phantom was used. This phantom is a flow phantom which is used for calibration and quality assurance in MRI perfusion studies using ASL pulse sequences. It simulates the head and neck region and the delivery of the labelled blood to the brain. The phantom's labelling chamber simulates a human neck where the upstream labelling of arterial blood is normally done during brain perfusion studies although complete labelling is also done for specific ASL techniques. A liquid which has a T1 of 1700 ms is used as the perfusate. The liquid then enters the perfusion chambers through a set of 60 arterioles arranged in a circular fashion which leads to a toroidal perfusion disc. The perfusion chamber consists of a stack of 6 discs made up of ultra high molecular weight polyethylene(UHMWPE) each measuring 4.75mm in thickness and 116 mm in diameter. The dimensions of the labelling and perfusion chambers are constructed so as to roughly mimic the arterial transit time in humans which is around 0.5 – 1.5 s according to the flow rate that is set from 100 to 400 ml/min (A Oliver-Taylor, 2019). At a flow rate of 350 ml/min, the perfusion values range anywhere between 500-600 ml/min/100g . To setup the phantom unit inside the scanner (Siemens), appropriate foaming pads were used so as to align the laser marker crosshairs just below the perfusion chamber of the phantom, and the Field of View was set appropriately so that the whole perfusion chamber was covered.

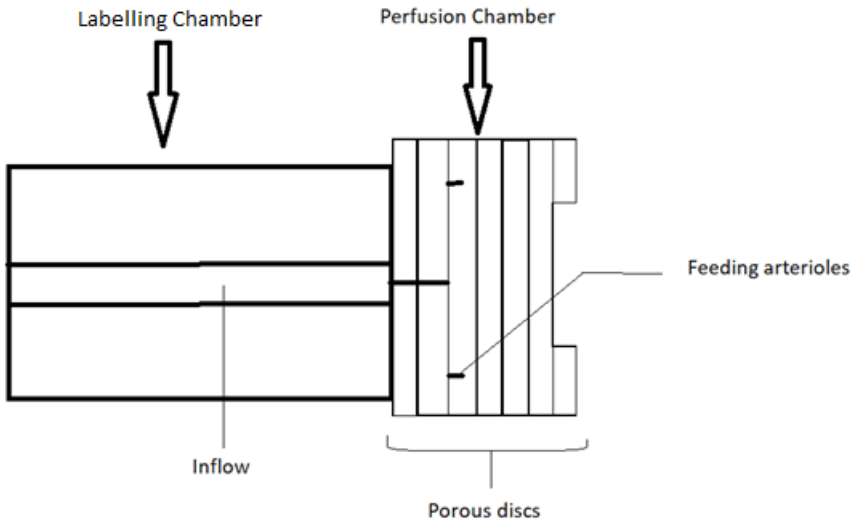

Figure:9 Schematic Digram of the QASPER Phantom

3.1 Pulse sequence and Image Acquisition:

A FAIR PASL Pulse sequence was used. It incorporated the QUIPSII saturation pulses in order to cut off the trailing bolus edges to get a well defined bolus. A turbo gradient spin echo sequence was used in the Siemens Prisma scanner with a Field Strength of 3T, a TR of 7310 ms, TI of 1990ms, the QUIPSSII pulse/TI1 at 700 ms and slice thickness of 3mm. The control image was taken as a reference M0 like image in this study. Flow rates(in ml/min) of 100 , 200, 300, 400, 450 and 485 were used separately in each imaging session. The control and label images were acquired in an interleaved manner with the slice selection turned on for the Label and turned off for the Control Images. Figure :8 depicts the pulse sequence.

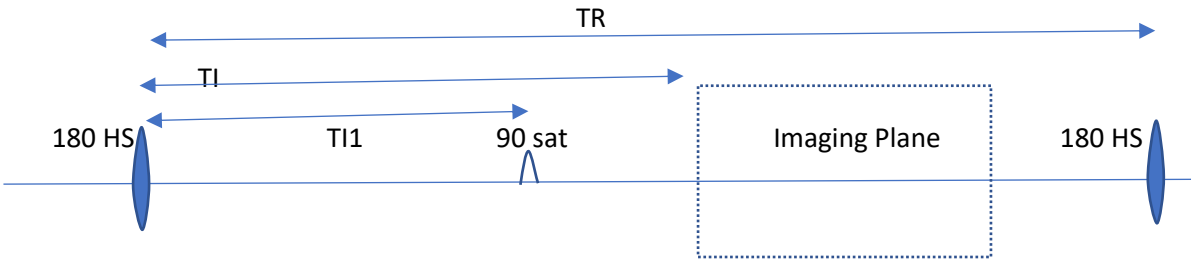

Figure:10 FAIR PASL pulse sequence. A hyperbolic secant pulse provides inversion of spins. The QUIPSS II pulse is the 90 degree saturation pulse.

3.2 Data Processing:

The acquired data were processed using spm12 and MATLAB. The images were first converted from nifty to dicom format using SPM12. As the phantom, unlike a patient, was still and not subject to any movement, there were no pre-processing steps needed for the sets of dicom images like Coregistration, normalization and smoothening and were hence skipped. The Control and label images were subtracted to get a difference/perfusion image (ΔM) . The Labelled bolus reduces the local magnetization and gives rise to a lower signal as compared to the control images where the spins are along the direction of B1. This was used to identify roughly, the regions of perfusion in the difference image. The figure:9 below shows the results of voxel wise subtraction. It can be seen that from figure:11 that there is a bright perfusion ring(inner ring) in the resulting difference image which was taken to analyze the perfusion. Figure:13 shows the region of interest in the perfusion image for which a binary mask was subsequently created.

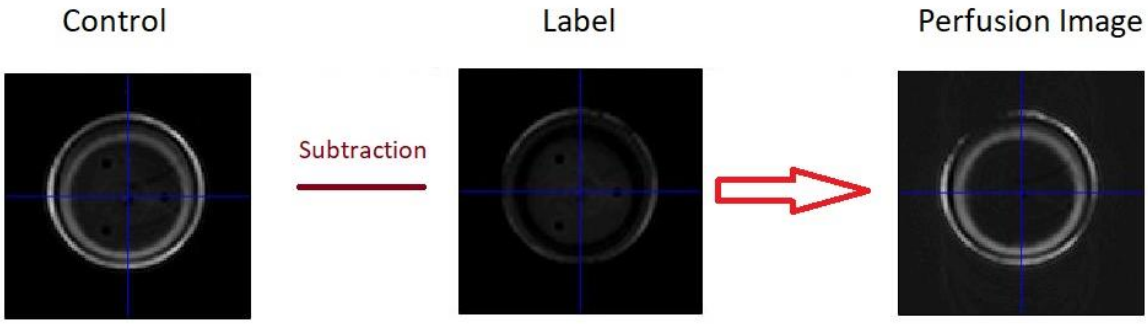

Figure:11 Voxelwise subtraction of the Control and the Labelled Image resulting in the ΔM image

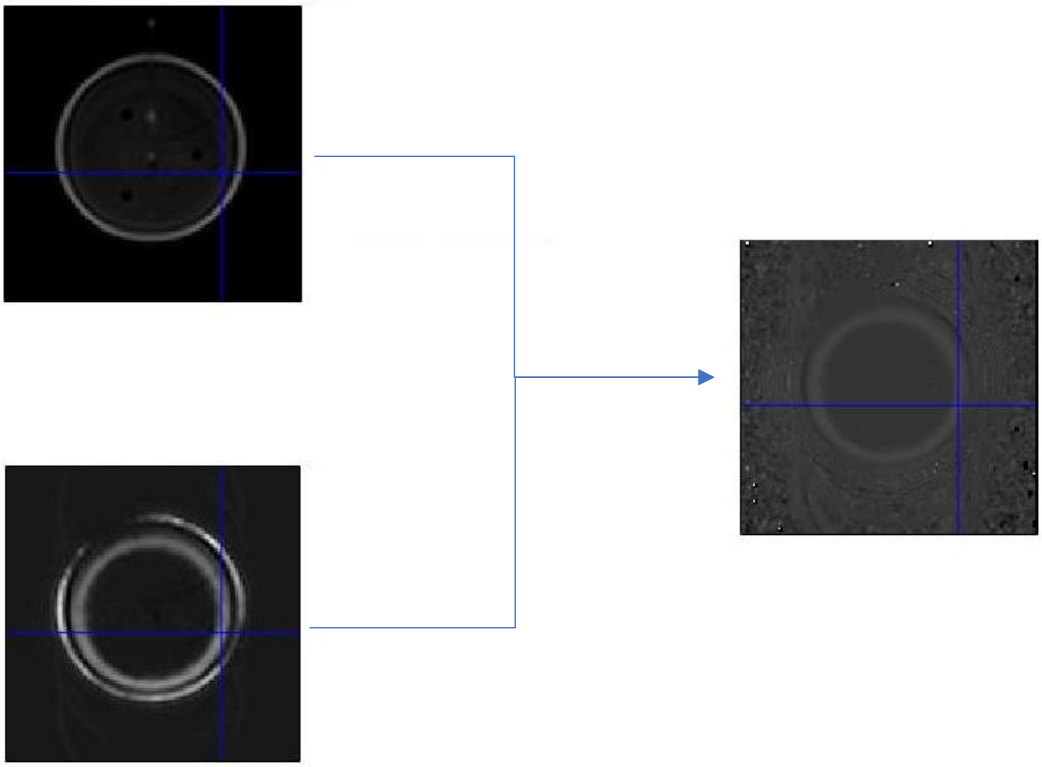

Figure:12 Ratio Image formed from *voxelwise division of ΔM by M0.*

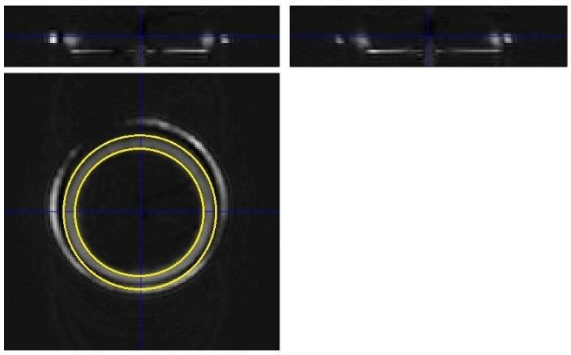

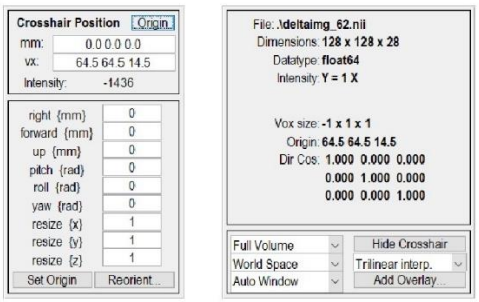

Figure:13 The Perfusion image with the highlighted torroidal19 region .

3.3 ROI Creation:

In order to specifically analyze the perfusion ring region, a toroidal mask was made so that it matches the region of interest. Two binary ring masks were made one of 20 and another of 25 voxel radii. These were then multiplied which resulted in a 20toroidal ring of 5 voxel thickness. The equation is the solution for the radius of a circle , which was used as conditions to get the circles of the desired radius. The mask resulted in binary values of 1 and 0 with the intensities inside the toroid being 1 and the background being 0.

$$\sqrt{(x-a)^2+(y-b)^2} = r \text{.....(10)}$$

Where,

(x,y) are the coordinates of the center of the phantom with x=64.5 and y=64.5.

(a,b) are points inside the circle.

R is the radius.

Perfusion Disc Selection:

Each perfusion disc in the QASPER phantom is 4.75 mm in thickness. As the slice thickness during acquisition was set at 3mm, the 6 discs were roughly divided into 10 slices in the image with the slice numbers ranging from 10 to 19. The created ROI mask was then multiplied to the ratio image. After applying the quantification formula to the ROI, an approximate perfusion map was derived over which, the CBF calculations were quantified.

Quantification:

The CBF formula from equation:8 that was used in the white paper which is an adaptation of the General Kinetic Model was used.

$$CBF = \frac{6000 \cdot \lambda . \Delta M . e^{\left(TI/T_{1p}\right)}}{2 \cdot \alpha . TI1 . M0}$$

Where, the term ΔM/M0, corresponds to the Ratio image. TI was set at 1990 ms, T1 is the T1 of perfusate which was 1900ms. TI1 is the bolus duration which was set at 700ms. The partition coefficient λ was set at 0.32 as stated in the QASPER documentation (A Oliver-Taylor, 2019) and the tagging efficiency α for PASL is 0.98.. The final colour coded image used for analysis is shown below in figure:14. The global CBF values were then calculated for each slice and its corresponding flow rates along with the ΔM signal intensities.

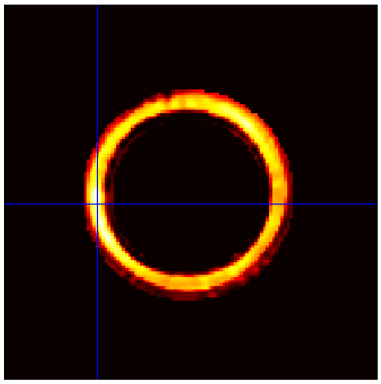

Figure:14 CBF map showing the perfusion disc of a selected slice.

4.0 Results and Discussion:

The results from the phantom study, showed that there was a lot of variability between the calculated perfusion values and the results deviated by a large margin from the values stated in the documentation. The graph in figure:16 shows the perfusion trend, across the different slices. The table of results from figure:16 & 17 show a high degree of variability in the calculated perfusion values within the 9 (slice numbers 10-19) owing to the relaxation effect. Flow rate of 100 ml/min showed no perfusion signal. There was some consistency around the feeding arterioles between slice numbers 12-14. Figure:18, shows the trend in the ratio (ΔM/M0) images which reflects in the amount of ASL signal that was acquired. The trend follows similarly to that shown previously with the perfusion. While the perfusion increased as the flow rates were increased from 100 ml/min to 400 ml/min, a slight drop was observed past that. The CBF maps showed areas of low signal especially for flow rates of 450 ml/min and 485 ml/min. This could have been due to draining of the bolus. For this, voxels were selected in the regions of the perfusion map shown in figure:19 in regions showing low(ROI:1) and high(ROI:2) perfusion regions. The graphs in figure:20 show the perfusion in the regions.

The reason for the perfusion being zero for flow rate 100ml/min could be because of the fact that the bolus had not reached the imaging slice yet leading to no difference in the control and label images leading to a ΔM value of 0. Another necessity for this pulse sequence is that TI – TI1 > Transit time. In the case of flow rate 100 ml/min, the transit time is around 1.5 seconds and the value of TI – TI1 is 1290 ms. The reason for the quantified perfusion values being so high can be reasoned with Fig:17, which shows the ratio of the signal between ΔM and M0. While PASL signals, typically have a very small fraction of around 1 % of the labelled blood(perfusate), these ratio values are also significantly less than those shown in the graph. It can be seen that it is much higher from the graph with around 20 % for 200 ml/min flow rate to around 83% for 400 ml/min flow rate. This clearly indicates that the M0 used which was the averaged control images, was not a good approximation for an M0 image and that a separate M0 image is needed for scaling and for absolute quantification. Typically in most ASL studies, a proton density image with a relatively long TR of more than 5 seconds is used for acquiring M0. While the drop in the signal away from the arterioles (slices 13 and 14), can be related to the drop in the signal due to the relaxation effect of spins, the drop is more steep above the arterioles (discs 3, 4, 5, 6) than below (discs 1 & 2). This could be due to the flow

dynamics inside the phantom. A rough assumption of how the flow could be is shown in shown in fig:15(a). As the bolus enters from the disc 2, it moves both transversely and radially. The perfusates moves above and directly get drained but the perfusate below the arterioles has to travel to the sides and upwards as the draining outlet is located on the top and as it cannot exit anywhere below. Due to this, incoming spins can fill up the labelled bolus leaving discs 1 and 2 which could lead to a build up, causing an increase in the signal in the slices below. From the voxel analysis done as depicted in figure:19 for possible draining mentioned previously, it is seen that with the bright regions with high perfusion(ROI:2), there is a small increase in the values for 450 ml/min and 485 ml/min. But the values for the region shown in ROI:1, shows a greater drop in the signal due to which the overall effect is taken over by the draining leading to the small drop in the perfusion values after 400 ml/min flow rate. This leads to a less steeper drop below the arteriole.

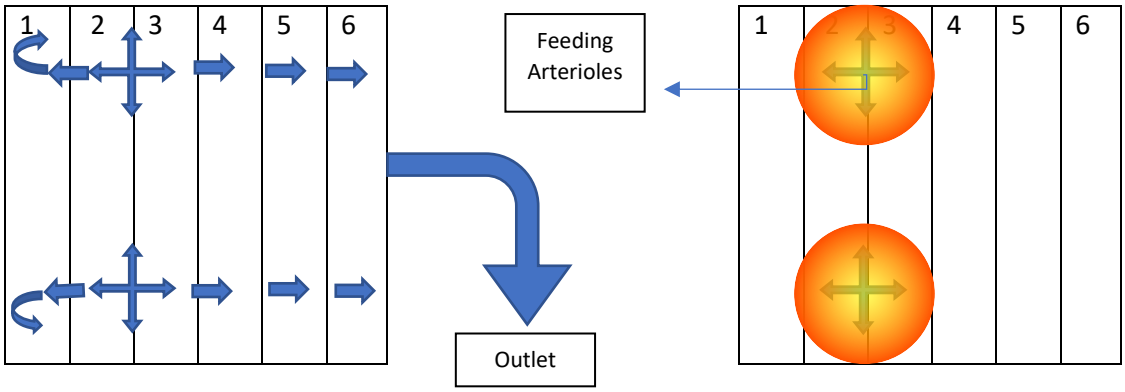

Figure:15 (a)Flow representation inside the phantom from the feeding arteries (b) shows the decrease in the tagged bolus as it perfuses through the perfusion discs.

Flow Rate(ml/min)	100	200	300	400	450	485
Slice10	0	2569	4178	11457	9866	9749
Slice11	0	2275	4069	12035	10980	10691
Slice12	0	3026	4478	14562	13431	12863
Slice13	0	3949	5373	16258	14418	13448
Slice14	0	3190	5259	15711	14372	13573
Slice15	0	733	2834	8827	7659	7293
Slice16	0	145,4	1309	4042	2962	2716
Slice17	0	0,54	600	1761	772	551
Slice18	0	0	417	1206	261	86
Slice19	0	0	171	463	1.8	0

Figure:16 Global Voxel intensities in ml/100g/min calculated across different slices for flow rates.

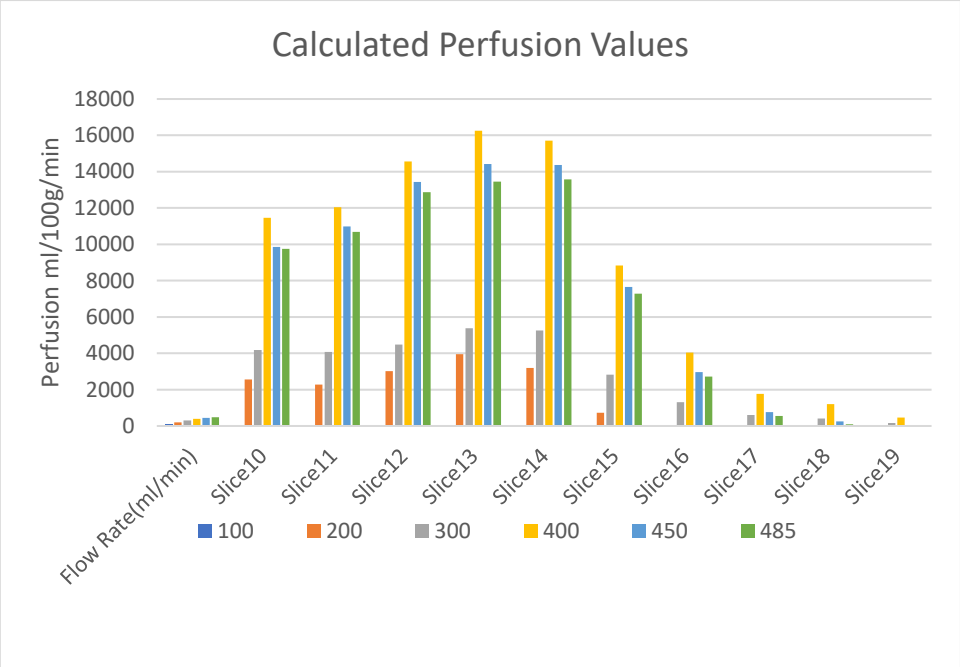

Figure:17 Graph representing the calculated perfusion rate for each flow rate across the slices

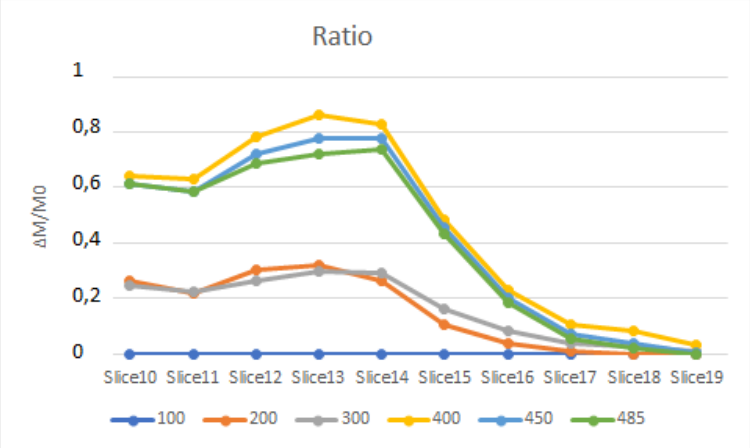

Figure:18 Graph representing the calculated perfusion rate for each flow rate across the slices

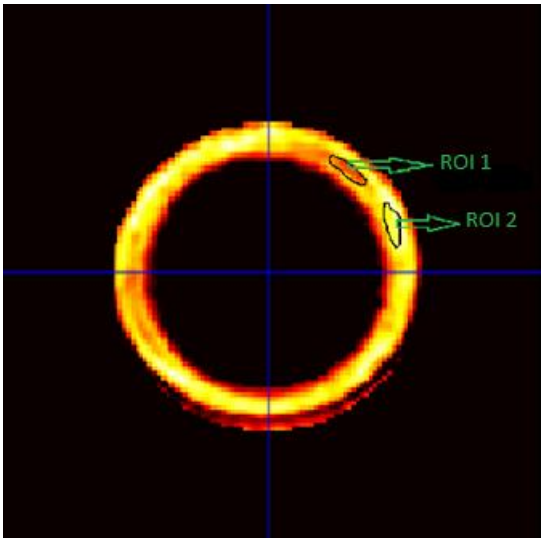

Figure:19 ROIs created for checking the loss in perfusion for the higher flow rates of 450 and 485 ml/min

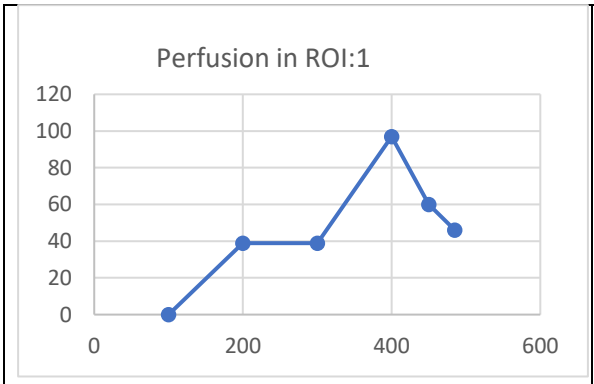

(a)

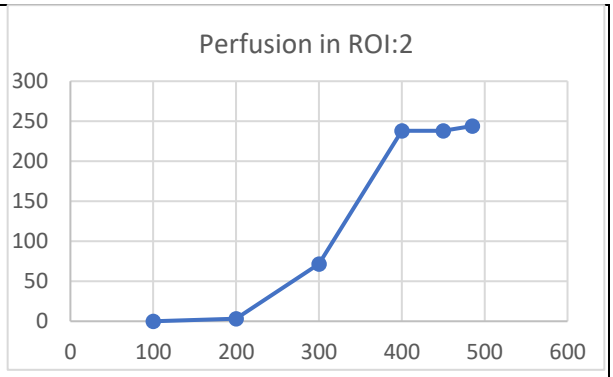

(b)

Figure:20(a) and (b) show the signal intensities in slice 13 for the ROIs in figure:19. The drop in signal, is due to the draining bolus which decreases the overall calculated perfusion for flow rates 450 ad 485 ml/min

5.0 Conclusion and Future Work:

The main goal of this study was to apply and validate the feasibility of the PASL FAIR pulse sequence incorporated with QUIPSS II ,with the set parameters in the quantification of perfusion on the QASPER phantom. Although the results suggest that the set parameters do not yield the results as mentioned in the documentation, there is a strong case with respect to the trend seen in the graph which relate to the flow dynamics within the phantom. Furthermore, although the parameters were set in line with the white paper, the fact that a proper M0 image was not used is another cause for the results deviating. Hence, the need for a proper M0 image is imperative as this study used the control as replacement and as the ratio of ΔM/M0 is a major scaling factor for quantification. This research also outlines the need for a separate estimation of the arterial transit time which will affect the timing of the QUIPSS II pulse, which will directly lead to the TI1 being different. A longer TI1 can be taken so as to allow the bolus in all the flow rates to be able to reach the imaging plane. With respect to the setup of the QASPER Phantom, the results suggest estimation of perfusion at the point of the feeding arteries or above perfusion disc 2 would lead to results that are less prone to error owing to the assumption, that there is possible re-entry of the bolus back into the first two discs causing a buildup. The graph also seems be relatable to the signal loss with respect to the relaxation of the spins which seems to be exponential only for values close to and above the feeding artery. Furthermore, the phantom documentation where a study comparing PASL and PCASL, also showed that the quantified values in PASL was significantly different that in pCASL (A.Oliver-Taylor, T.Hampshire, 2019)which indicates further tests to be done with the Phantom so as to come up with better reproducibility of results.

Future work can be done on the above issues. Firstly the temporal SNR can be calculated to analyze the voxel wise perfusion in each slice to see the stability of the flow within the phantom. The same experiment can be repeated with a proper M0 image and the results can be compared. The drawback of an unknown transit time, can be tackled through techniques like the Multi TI PASL, which has been shown to be useful in calculating the Arterial transit time. Once this is known, further investigations can be done to solve the problems of backflow in discs 1 & 2 in the phantom. With proper control of temporal length of the bolus, it can be possible that first, the labelled bolus is allowed to enter and then the ATT can be used to exactly know when then bolus would arrive at the layers below the feeding artery and this can be used to discard the backflow that happens as the perfusate is continuously pumped. Furthermore, the nature of the flow inside the phantom must be studied by calculating temporal deviations in the voxel signals to be able to come up with a flow rate range within which the flow is stable.

6.0 Ethics:

Arterial Spin Labelling uses the body's own blood water protons, to get the signals. In this research, no human trials were done as the phantom was the sole equipment used for measuring the signal and acquiring images. The data was collected in the 3 T Siemens scanner at the Universtiet Medisch Centrum Groningen (UMCG), under supervised environment. Standard procedures and protection protocols were followed while acquiring the data from the phantom. This study with further experiments and data can yield to a better calibration of the phantom which can be used as reference for calculating perfusion and scaling the values appropriately using ASL techniques in patients in the future. With proper scaling and calibration done, this can be used for studying perfusion in patients for various pathologies like tumours, fMRI studies in psychology and for various neuro-degenerative diseases.

7.0 References

A.Oliver-Taylor, T.Hampshire, H. J. M. (2019). A multi-site round-robin assessment of ASL using a perfusion phantom. *ISMRM 27th Annual Meeting and Exhibition*.

A Oliver-Taylor. (2019). *QASPER:Instructions for use*. https://goldstandardphantoms.com/sites/default/files/attachments/QASPER Instructions For Use 2019-07-08.pdf

Alsaedi, A., Thomas, D., Bisdas, S., & Golay, X. (2018). Overview and Critical Appraisal of Arterial Spin Labelling Technique in Brain Perfusion Imaging. *Contrast Media & Molecular Imaging*, *2018*, 5360375. https://doi.org/10.1155/2018/5360375

Alsop, D C, & Detre, J. A. (1998). Multisection cerebral blood flow MR imaging with continuous arterial spin labeling. *Radiology*, *208*(2), 410–416. https://doi.org/10.1148/radiology.208.2.9680569

Alsop, David C, Detre, J. A., Golay, X., Günther, M., Hendrikse, J., Hernandez-Garcia, L., Lu, H., MacIntosh, B. J., Parkes, L. M., Smits, M., van Osch, M. J. P., Wang, D. J. J., Wong, E. C., & Zaharchuk, G. (2015). Recommended implementation of arterial spin-labeled perfusion MRI for clinical applications: A consensus of the ISMRM perfusion study group and the European consortium for ASL in dementia. *Magnetic Resonance in Medicine*, *73*(1), 102–116. https://doi.org/https://doi.org/10.1002/mrm.25197

Berger, A. (2002). Magnetic resonance imaging. *BMJ (Clinical Research Ed.)*, *324*(7328), 35. https://doi.org/10.1136/bmj.324.7328.35

Buckley, D. L. (2002). Uncertainty in the analysis of tracer kinetics using dynamic contrast-enhanced T1-weighted MRI. *Magnetic Resonance in Medicine*, *47*(3), 601–606. https://doi.org/10.1002/mrm.10080

Buxton, R. B., Frank, L. R., Wong, E. C., Siewert, B., Warach, S., & Edelman, R. R. (1998). A general kinetic model for quantitative perfusion imaging with arterial spin labeling. *Magnetic Resonance in Medicine*, *40*(3), 383–396. https://doi.org/10.1002/mrm.1910400308

Calamante, F. (2010). Perfusion MRI Using Dynamic-Susceptibility Contrast MRI: Quantification Issues in Patient Studies. *Topics in Magnetic Resonance Imaging*, *21*(2). https://journals.lww.com/topicsinmri/Fulltext/2010/04000/Perfusion_MRI_Using_Dynamic_Susceptibility.3.aspx

Calamante, F., Gadian, D. G., & Connelly, A. (2000). Delay and dispersion effects in dynamic susceptibility contrast MRI: Simulations using singular value decomposition. *Magnetic Resonance in Medicine*, *44*(3), 466–473. https://doi.org/https://doi.org/10.1002/1522-2594(200009)44:3<466::AID-MRM18>3.0.CO;2-M

Chikui, T., Obara, M., Simonetti, A., Ohga, M., Koga, S., Kawano, S., Matsuo, Y., Kamintani, T., Shiraishi, T., Kitamoto, E., Nakamura, K., & Yoshiura, K. (2012). The Principal of Dynamic Contrast Enhanced MRI, the Method of Pharmacokinetic Analysis, and Its Application in the Head and Neck Region. *International Journal of Dentistry*, *2012*, 480659. https://doi.org/10.1155/2012/480659

Dai, W., Garcia, D., de Bazelaire, C., & Alsop, D. C. (2008). Continuous flow-driven inversion for arterial spin labeling using pulsed radio frequency and gradient fields. *Magnetic Resonance in*

Medicine, *60*(6), 1488–1497. https://doi.org/10.1002/mrm.21790

Edelman, R. R., Siewert, B., Darby, D. G., Thangaraj, V., Nobre, A. C., Mesulam, M. M., & Warach, S. (1994). Qualitative mapping of cerebral blood flow and functional localization with echo-planar MR imaging and signal targeting with alternating radio frequency. *Radiology*, *192*(2), 513–520. https://doi.org/10.1148/radiology.192.2.8029425

Fantini, S., Sassaroli, A., Tgavalekos, K. T., & Kornbluth, J. (2016). Cerebral blood flow and autoregulation: current measurement techniques and prospects for noninvasive optical methods. *Neurophotonics*, *3*(3), 31411. https://doi.org/10.1117/1.NPh.3.3.031411

Ferré, J.-C., Bannier, E., Raoult, H., Mineur, G., Carsin-Nicol, B., & Gauvrit, J.-Y. (2013). Arterial spin labeling (ASL) perfusion: Techniques and clinical use. *Diagnostic and Interventional Imaging*, *94*(12), 1211–1223. https://doi.org/https://doi.org/10.1016/j.diii.2013.06.010

Gevers, S., Nederveen, A. J., Fijnvandraat, K., van den Berg, S. M., van Ooij, P., Heijtel, D. F., Heijboer, H., Nederkoorn, P. J., Engelen, M., van Osch, M. J., & Majoie, C. B. (2012). Arterial spin labeling measurement of cerebral perfusion in children with sickle cell disease. *Journal of Magnetic Resonance Imaging : JMRI*, *35*(4), 779–787. https://doi.org/10.1002/jmri.23505

Grover, V. P. B., Tognarelli, J. M., Crossey, M. M. E., Cox, I. J., Taylor-Robinson, S. D., & McPhail, M. J. W. (2015). Magnetic Resonance Imaging: Principles and Techniques: Lessons for Clinicians. *Journal of Clinical and Experimental Hepatology*, *5*(3), 246–255. https://doi.org/10.1016/j.jceh.2015.08.001

Hawkes, R. C., Holland, G. N., Moore, W. S., & Worthington, B. S. (1980). Nuclear Magnetic Resonance (NMR) Tomography of the Brain: A Preliminary Clinical Assessment with Demonstration of Pathology. *Journal of Computer Assisted Tomography*, *4*(5). https://journals.lww.com/jcat/Fulltext/1980/10000/Nuclear_Magnetic_Resonance__NMR__Tomography_of_the.1.aspx

Jahng, G.-H., Li, K.-L., Ostergaard, L., & Calamante, F. (2014). Perfusion magnetic resonance imaging: a comprehensive update on principles and techniques. *Korean Journal of Radiology*, *15*(5), 554–577. https://doi.org/10.3348/kjr.2014.15.5.554

Kim, S.-G. (1995). Quantification of relative cerebral blood flow change by flow-sensitive alternating inversion recovery (FAIR) technique: Application to functional mapping. *Magnetic Resonance in Medicine*, *34*(3), 293–301. https://doi.org/https://doi.org/10.1002/mrm.1910340303

Kwong, K. K., & Chesler, D. A. (1997). *The MR T1 Based Perfusion Model BT - Optical Imaging of Brain Function and Metabolism 2: Physiological Basis and Comparison to Other Functional Neuroimaging Methods* (A. Villringer & U. Dirnagl (eds.); pp. 27–34). Springer US. https://doi.org/10.1007/978-1-4899-0056-2_3

Luh, W.-M., Wong, E. C., Bandettini, P. A., & Hyde, J. S. (1999). QUIPSS II with thin-slice TI1 periodic saturation: A method for improving accuracy of quantitative perfusion imaging using pulsed arterial spin labeling. *Magnetic Resonance in Medicine*, *41*(6), 1246–1254. https://doi.org/https://doi.org/10.1002/(SICI)1522-2594(199906)41:6<1246::AID-MRM22>3.0.CO;2-N

Nery, F., Buchanan, C. E., Harteveld, A. A., Odudu, A., Bane, O., Cox, E. F., Derlin, K., Gach, H. M., Golay, X., Gutberlet, M., Laustsen, C., Ljimani, A., Madhuranthakam, A. J., Pedrosa, I., Prasad, P. V, Robson, P. M., Sharma, K., Sourbron, S., Taso, M., … Fernández-Seara, M. A. (2020). Consensus-based technical recommendations for clinical translation of renal ASL MRI. *Magnetic Resonance Materials in Physics, Biology and Medicine*, *33*(1), 141–161. https://doi.org/10.1007/s10334-019-00800-z

Parker, G. J. M., Baustert, I., Tanner, S. F., & Leach, M. O. (2000). Improving image quality and T1 measurements using saturation recovery turboFLASH with an approximate K-space normalisation filter. *Magnetic Resonance Imaging*, *18*(2), 157–167. https://doi.org/https://doi.org/10.1016/S0730-725X(99)00124-1

Rosen, B. R., Belliveau, J. W., Vevea, J. M., & Brady, T. J. (1990). Perfusion imaging with NMR contrast agents. *Magnetic Resonance in Medicine*, *14*(2), 249–265. https://doi.org/https://doi.org/10.1002/mrm.1910140211

Stadler, K. L., Pease, A. P., & Ballegeer, E. A. (2017). Dynamic Susceptibility Contrast Magnetic Resonance Imaging Protocol of the Normal Canine Brain. *Frontiers in Veterinary Science*, *4*, 41. https://doi.org/10.3389/fvets.2017.00041

Tiwari, Y. V, Lu, J., Shen, Q., Cerqueira, B., & Duong, T. Q. (2017). Magnetic resonance imaging of blood-brain barrier permeability in ischemic stroke using diffusion-weighted arterial spin labeling in rats. *Journal of Cerebral Blood Flow and Metabolism : Official Journal of the International Society of Cerebral Blood Flow and Metabolism*, *37*(8), 2706–2715. https://doi.org/10.1177/0271678X16673385

van Osch, M. J. P., Vonken, E. P. A., Viergever, M. A., van der Grond, J., & Bakker, C. J. G. (2003). Measuring the arterial input function with gradient echo sequences. *Magnetic Resonance in Medicine*, *49*(6), 1067–1076. https://doi.org/10.1002/mrm.10461

Wang, J., Alsop, D. C., Li, L., Listerud, J., Gonzalez-At, J. B., Schnall, M. D., & Detre, J. A. (2002). Comparison of quantitative perfusion imaging using arterial spin labeling at 1.5 and 4.0 Tesla. *Magnetic Resonance in Medicine*, *48*(2), 242–254. https://doi.org/10.1002/mrm.10211

Williams, D. S., Detre, J. A., Leigh, J. S., & Koretsky, A. P. (1992). Magnetic resonance imaging of perfusion using spin inversion of arterial water. *Proceedings of the National Academy of Sciences*, *89*(1), 212 LP – 216. https://doi.org/10.1073/pnas.89.1.212

Wong, E. C., Buxton, R. B., & Frank, L. R. (1998). Quantitative imaging of perfusion using a single subtraction (QUIPSS and QUIPSS II). *Magnetic Resonance in Medicine*, *39*(5), 702–708. https://doi.org/https://doi.org/10.1002/mrm.1910390506

Zhang, N., Gordon, M. L., & Goldberg, T. E. (2017). Cerebral blood flow measured by arterial spin labeling MRI at resting state in normal aging and Alzheimer's disease. *Neuroscience & Biobehavioral Reviews*, *72*, 168–175. https://doi.org/https://doi.org/10.1016/j.neubiorev.2016.11.023